

# Preliminary Evaluation of Candidate Candle Filter Materials

Jack D. Spain (spain@sri.org)  
H. Stuart Starrett (starrett@sri.org)  
Southern Research Institute  
757 Tom Martin Drive  
Birmingham, Alabama 35211

## Introduction

Coal-fired Pressurized Fluidized Bed Combustion (PFBC) and Integrated Gasification Combined Cycle (IGCC) systems require ceramic candle filter elements that can withstand the mechanical, thermal, and chemical environment of hot gas cleanup applications. These systems require filter elements to sustain the thermal stresses of normal operations (pulse cleaning), of start-up and shut-down conditions, and of thermal transients generated during process upsets. They must have sufficient strength to withstand the mechanical loads associated with handling and assembly. For long-term operation, they must withstand the chemical environment of the PFBC system at temperatures up to 1600°F without chemical degradation, creep, or static fatigue failure.

Previous characterization of candidate candle filter materials has focused on Schumacher and Pall clay-bonded SiC and Coors P-100A-1 alumina mullite filters. Results obtained for the SiC materials indicate that up to 1400°F, these materials potentially have a long life (thousands of hours) in the absence of major process upsets and temperature excursions. Above 1400°F, creep, static fatigue, and property degradation will limit the use of clay-bonded SiC materials. Coors alumina mullite is not susceptible creep or property degradation; however, static fatigue and susceptibility to thermal stress failure, especially in the event of temperature excursions, will limit the use of this material.

Dupont/Lanxide PRD-66C, McDermott continuous fiber ceramic composite, Blasch Precision Ceramics 4-270 monolithic oxide ceramic, and Specific Surface cordierite have been manufactured in an effort to provide candle filters which can survive long term operation at temperatures up to 1600°F in the hot gas filtration environment of PFBC systems. Dupont/Lanxide PRD-66C is an all-oxide candle filter manufactured using a consumable textile grade glass yarn in an Al<sub>2</sub>O<sub>3</sub> binder. Two PRD-66C candle filters with dimensions of ~2.35" O.D. x ~1.74" I.D. x ~60" long were supplied for testing. McDermott continuous fiber ceramic composite is manufactured of continuous Nextel 610 fiber and chopped saffil fiber in an Al<sub>2</sub>O<sub>3</sub> binder. One McDermott candle filter with dimensions of ~2.36" O.D. x ~1.94" I.D. x ~60" long was supplied for testing. Blasch Precision Ceramics 4-270 is a mullite-bonded aluminum oxide monolithic ceramic. One Blasch candle filter with dimensions of ~2.36" O.D. x ~1.50" I.D. x ~60" long was supplied for testing. Specific Surface cordierite candles consist of two concentric filter walls, shaped like a sock with the toe end tucked back inside, connected by "stiffeners". The outer filter wall is ~2.40" O.D. x ~1.98" I.D. and the overall candle length is ~12.75". All testing was conducted on specimens taken from the outer wall of one candle filter. Preliminary evaluations have been conducted on the materials listed above in order to obtain an initial indication of the materials ability to operate in the hot

gas filtration environment. Properties measured include room temperature hoop tensile strength, room temperature axial tensile stress-strain response, thermal expansion from room temperature to ~1600°F, and thermal conductivity from room temperature to ~1600°F. Results obtained to date are presented in this paper.

## **Objectives**

Objectives of the test program at Southern Research are as follows:

1. Provide material characterization to develop an understanding of the physical, mechanical, thermal behavior of hot gas filter materials.
2. Develop a material property data base from which the behavior of materials in the hot gas cleanup environment may be predicted.
3. Perform testing and analysis of filter elements after exposure to actual operating conditions to determine the effects of the thermal and chemical environments in hot gas filtration on material properties.

## **Approach**

Based on the anticipated operating conditions in the hot gas cleanup environment and on the in-service performance of candle filters tested to date, several critical issues have been identified for candle filter materials. A summary of the critical material issues for candle filters is given in Table 1. As shown, material issues are summarized in four categories, installation and handling, pulse cleaning, process upsets, and life, which place different requirements on the candles. The candles must have sufficient strength to withstand the mechanical loads and “toughness” to withstand bumps, nicks, scrapes, etc. associated with handling and installation. During pulse cleaning, the backpulse imparts a temperature difference on the inside surface of the candle rapidly enough that the temperature distribution through the candle wall is nearly a step function. That is, the surface achieves the temperature of the backpulse gas while the rest of the material is still at the nominal operation temperature. Therefore, the thermal stress level during pulse cleaning is set by the candle operating temperature, backpulse gas temperature, Young’s modulus of the candle, and the thermal expansion of the candle while thermal diffusivity has little influence. During process upsets, the temperature changes over a period seconds or minutes so that the material through the wall thickness will react and heat up or cool down so that a more moderate gradient is obtained. The temperature gradients generated during process upsets will depend on the thermal diffusivity of the candle. Therefore, since the thermal stress level depends on the temperature gradient, the thermal stresses generated during process upsets will be set by the temperature rise/drop rate of the upset, Young’s modulus, thermal expansion, and thermal diffusivity of the candle. Long-term operation will require candle filters that can survive the thermal and chemical environment without creep or static fatigue failure or excessive property degradation due to chemical attack. Testing was conducted according to the test matrix shown in Table 2. This test matrix was designed to address the critical issues discussed above. For example, mechanical strength is addressed by tensile strength measurements while

thermal stress susceptibility is addressed by measuring tensile stress-strain, thermal expansion, and thermal conductivity measurements. There are several critical material issues not discussed above such as permeability, ability to manufacture to desired dimensions, cost, etc. These issues are not being addressed under the current test plan for these materials at Southern.

## Results

### Dupont/Lanxide PRD-66

Room temperature axial tensile stress-strain responses were measured on six specimens. Three specimens were machined from two different filter elements and the specimens were taken from various axial locations (that is, bottom, middle, and top). Each specimen consisted of a 7-inch long, full diameter section of the element. Two inches on each end of the specimens were used for gripping, leaving a three-inch long gage section. Strain was measured over a two-inch long region at the middle of the gage section. The responses were digitized and are shown in Figure 1 and the properties obtained are summarized in Table 3. Note that four of the specimens failed at the glue line at the end of the grips. Failure at the glue line appeared to have little affect on the ultimate strength or strain-to-failure; however, the values were not included in the calculation of averages. The average properties obtained were: ultimate tensile strength – 290 psi, Young’s modulus – 0.35 msi, and strain-to-failure – 1.65 mils/inch.

Room temperature hoop tensile properties were measured on eighteen specimens. Nine specimens were machined from various axial locations of two different candles. Strain gages were mounted to the inside and outside surfaces of four specimens both to try and obtain a measure of Young’s modulus in the hoop direction and to investigate the anisotropic behavior of the material. Note that some difficulty in using strain gages with this material is acknowledged. First, the surfaces are rough which leads to difficulty attaching the gages. Second, strain gage epoxy impregnates the pores and can affect the measured values. However, even with these difficulties the strain gages were used because it is necessary to understand the anisotropic nature of the material. For an isotropic material, hoop stresses are given by the classical elasticity equation for a thick-walled ring:

$$S_q = \frac{a^2 P}{b^2 - a^2} \left( 1 + \frac{b^2}{r^2} \right)$$

where:  $\Phi_2$  = hoop tensile stress  
P = uniform internal gage pressure  
a = inside radius  
b = outside radius

If the stresses are evaluated at the ID and OD, then a ratio of  $\frac{S_{q/ID}}{S_{q/OD}} = \frac{1}{2} \left( 1 + \frac{b^2}{a^2} \right)$

is obtained. Further, if the stress-strain response is linear, then  $\frac{e_{q/ID}}{e_{q/OD}} = \frac{1}{2} \left( 1 + \frac{b^2}{a^2} \right)$

For the PRD-66C rings tested, the ratio of  $\frac{e_{q/ID}}{e_{q/OD}}$  was calculated to be 1.2 for the isotropic stress distribution. However, results obtained from the strain gages showed that  $\frac{e_{q/ID}}{e_{q/OD}} \sim 3.5$ . These results indicate that the PRD-66C material is anisotropic. The equation for maximum stress in an anisotropic thick-walled ring is given by (see Lekhnitskii, Reference 1):

$$S_q = \frac{P_i k \left( \frac{a}{b} \right)^{k+1}}{1 - \left( \frac{a}{b} \right)^{2k}} \left[ \left( \frac{a}{b} \right)^{k-1} + \left( \frac{b}{a} \right)^{k+1} \right]$$

where  $\Phi_2, P_i, a,$  and  $b$  are as defined above and  $k = \sqrt{\frac{E_q}{E_r}}$

The hoop tensile properties are summarized in Table 4. Strength values are shown as calculated by the isotropic solution and the anisotropic solution while Young's modulus values shown were all calculated by the anisotropic analysis. Since only four strain gaged specimens have been tested, the anisotropic values should be considered preliminary until more strain gage data are obtained. Average properties were: ultimate tensile strength – 840 psi by isotropic solution and 1400 psi by anisotropic solution, Young's modulus – 3.0 msi, and hydrostatic pressure at failure – 240 psig.

Axial and diametral thermal expansions are plotted in Figure 2. A secant coefficient of thermal expansion (CTE) between 500 °F and 1500 °F was calculated for the axial direction and a value of  $2.2 \times 10^{-6}/^{\circ}\text{F}$  was obtained. The CTE was calculated over this temperature range because it is likely that pulse cleaning and most thermal transients would occur within this range. The diametral expansion plotted in Figure 2 represents the change in diameter divided by the initial diameter. For anisotropic materials, thermal stresses are generated by temperature changes and these stresses restrain the specimen from its free expansion. Therefore, the expansion shown represents a structural value, not a material property. That is, the values would be different if the dimensions (ID and OD) were different.

### McDermott Ceramic Composite

Room temperature and tensile stress-strain responses were measured on three specimens taken from various axial locations of one filter element. Specimen and loading configurations were like those used for PRD-66C. The responses were digitized and are shown in Figure 3 and the properties obtained are summarized in Table 5. Note that one specimen failed in the grip section. This was the first specimen tested and it was determined that failure occurred in the grip due to insufficient epoxy impregnation. For the two subsequent tests, better epoxy impregnation was obtained and failure occurred in

the gage. The values shown in Table 5 for ultimate tensile strength and strain-to-failure correspond to the endpoints shown in Figure 3 and represent the point where maximum load was measured. The specimen did continue to carry some load and strain beyond this point; however, it is likely that damage had occurred which would render the material ineffective as a filter. To determine the damage level this material could withstand and still operate effectively would require additional work. Based on the endpoints as shown in Figure 3, properties obtained were: ultimate tensile strength – 610 psi, Young’s modulus – 0.45 msi, strain-to-failure – 2.1 mils/inch.

Hoop tensile tests were conducted on one-inch high rings but the ultimate strength was not obtained because fiber pullout rather than tensile failure occurred. Additional longer specimens were not tested because all material had been consumed for other test specimens. Longer specimens will be tested when more material becomes available.

Axial and diametral thermal expansions are plotted in Figure 4. The secant CTE between 500EF and 1500EF was  $4.6 \times 10^{-6}$  in./in./EF. As with PRD-66C, the diametral expansion shown in Figure 4 includes the effect of thermal stresses generated due to differences in radial and hoop thermal expansion.

#### **Blasch Precision Ceramics 4-270**

Room temperature and tensile stress-strain responses were measured on four specimens taken at one axial location of one candle filter. Two additional specimens failed during machining. Unlike PRD-66C and McDermott, these specimens were taken from the wall of the candle filter and machined to a cylindrical, dogboned shape. Overall specimen length was 4.1 inches with the gage dimensions were 0.25” dia. x 1.20” long. The stress-strain responses obtained were digitized and are shown in Figure 5 and the properties obtained are summarized in Table 6. As shown, considerable variability was seen. Average properties were: ultimate tensile strength – 250 psi, Young’s modulus – 0.80 msi, strain-to-failure – 0.30 mils/inch.

Room temperature tensile hoop strength was measured on nine specimens machined from various axial locations of one filter element. Values obtained were calculated from the elasticity solution for isotropic, thick-walled rings. Although it was not verified that this material is isotropic, there were no reasons to suspect anisotropy. The wall of each specimen had relatively thick and thin sections and all calculations were based on an average thickness. Hoop tensile results are summarized in Table 7. Average values were: ultimate tensile strength - 440 psi and hydrostatic pressure at failure – 180 psig. These average values do not include results obtained from specimens Tn-Hoop-1, 2, and 3. These specimens all came from the same region near the closed end of the filter. One of these specimens broke in handling and the other two failed at stress levels well below the other six specimens.

Axial thermal expansion is plotted in Figure 6. The secant CTE between 500EF and 1500EF was  $4.1 \times 10^{-6}$  in./in./EF.

## Specific Surface Cordierite

Room temperature hoop tensile strength was measured on four specimens, two taken from near the flanged end of the candle and two taken from near the opposite end. The results are summarized in Table 8. Two ultimate strength values, 370 psi and 270 psi, were obtained and the corresponding values of hydrostatic pressure at failure were 70 psig and 53 psig. The other two specimens failed at very low stress levels. However, these specimens were taken from the region of the candle where “stiffeners” connect the inner and outer filter walls. The connection of the stiffeners to the candle wall likely served to reduce the strength of these two specimens so that these values do not represent the strength of the material. During service, the stiffeners may cause stress or strain intensification.

Axial thermal expansion is plotted in Figure 7. The secant CTE between 500EF and 1500EF was  $1.0 \times 10^{-6}$  in./in./EF.

## Material Comparisons

Probable value axial, room temperature stress-strain curves for Dupont/Lanxide PRD-66C, McDermott ceramic composite, and Blasch 4-270 are plotted in Figure 8 along with previously reported curves for Pall 326, Schumacher TF20, and Coors P-100A-1. All the new materials had lower strengths than Pall, Schumacher, or Coors. However, PRD-66C and McDermott ceramic composite had much greater strain-to-failure which may lead to a tougher material more likely to survive thermal stresses generated during process transients. Room temperature tensile strengths in both the axial and hoop directions (where available) are compared for several materials in as-manufactured condition in Figure 9. This figure illustrates the lower as-manufactured strengths of the new materials. Several additional issues including material variability and property degradation during service should be addressed by future testing. Axial thermal expansion is plotted for the same seven materials in Figure 10. This figure shows McDermott ceramic composite and Blasch 4-270 have thermal expansion approaching the literature values for alumina with CTE values of  $4.6 \times 10^{-6}$  in./in./EF and  $4.1 \times 10^{-6}$  in./in./EF, respectively. Pall 326, Schumacher TF20, Coors P-100A-1, and Dupont PRD-66C and similar thermal expansions with CTE values ranging from  $2.2 \times 10^{-6}$  in./in./EF for Pall 326 and Coors P-100A-1. Specific surface cordierite has the lowest expansion with a CTE of  $1.0 \times 10^{-6}$  in./in./EF. Some key properties of several candle filter materials are compared in Table 9.

## Conclusions

Dupont/Lanxide PRD-66C and McDermott ceramic composite have lower tensile strength than previously tested Pall 326 or Coors P-100A-1. The McDermott material has a strength comparable to Schumacher TF20 while PRD-66C is weaker. However, both materials had a strain-to-failure of approximately 3 times Coors P-100A-1 and an order of magnitude greater the clay-bonded SiC materials. The combination of tensile strain-to-failure and thermal expansion indicates that both PRD-66C and the McDermott material may withstand more severe temperature gradients than the previously tested

materials. Thermal conductivity measurements are needed to evaluate the ability of these materials to survive during process upsets. Also, additional testing is needed to address life issues including creep and property loss during service for PRD-66C and McDermott ceramic composite.

Blasch 4-270 had a lower tensile strength than the previously tested materials and a strain-to-failure similar to Pall 326 and Schumacher TF20. Thermal expansion was higher than the clay-bonded SiC or Coors alumina mullite materials. The all-oxide composition may lead to better chemical compatibility in the PFBC environment than clay-bonded SiC; however, the combination of low strength and strain-to-failure with high thermal expansion may lead to problems surviving process upsets.

Specific Surface cordierite was manufactured and tested under this program both to evaluate a manufacturing technique and to investigate the use of cordierite as a candle filter material. The limited testing completed so far on this material indicates a reasonable tensile strength, although lower than for most other candle materials tested, and the lowest thermal expansion of any candle tested so far were obtained.

### **Future Plans**

Future plans at Southern include:

- complete testing shown in the test matrix for PRD-66C, McDermott ceramic composite, Blasch 4-270, and Specific Surface cordierite (more PRD-66C and McDermott material are required).
- measure residual properties after service in PFBC to address long-term survivability.
- perform testing on additional materials as they become available.

### **Reference**

1. Lekhnitskii, S.G., Anisotropic Plates, Gordon and Breach Science Publishers, 1968.

### **Acknowledgments**

This research was sponsored by the U.S. Department of Energy's Federal Energy Technology Center, under Contract DE-AC-21-94MC31160 with Southern Research Institute, P.O. Box 55305, Birmingham, Alabama 35255-5305. We wish to acknowledge FETC Contracting Officer Representative Mr. Theodore J. McMahon and also Mr. Richard Dennis of FETC for their technical support during this program. We also wish to acknowledge Mr. Howard Hendrix and his staff at Southern Company Services for their help in understanding the PFBC environment.

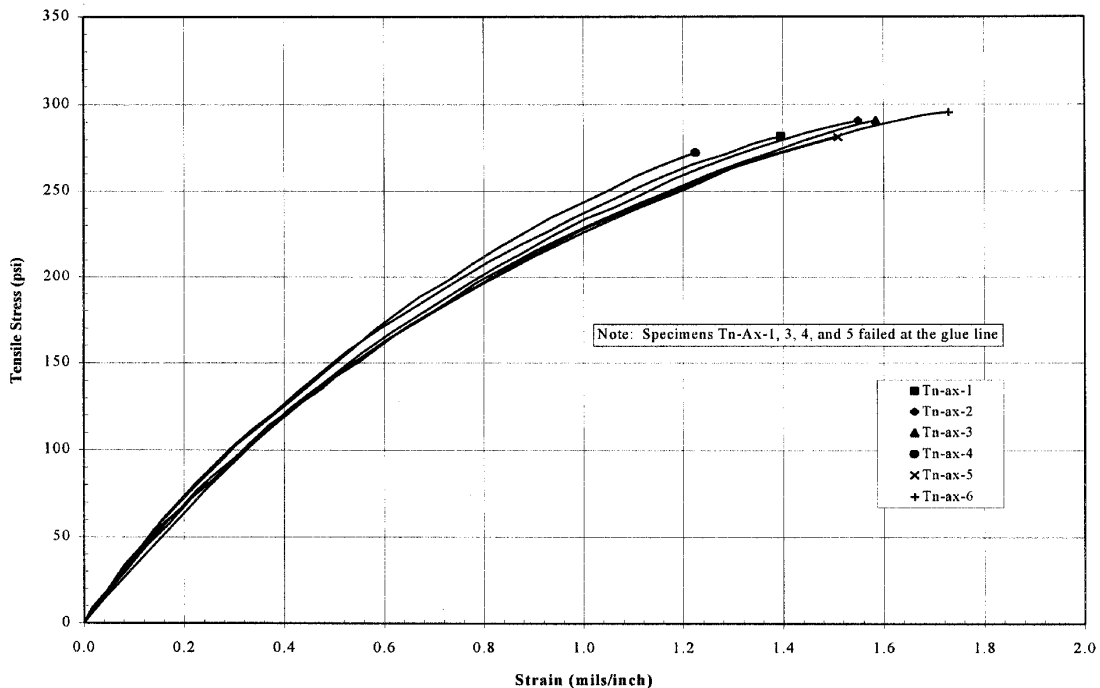


Figure 1. Axial Tensile Stress-Strain Responses for Dupont/Lanxide PRD-66C

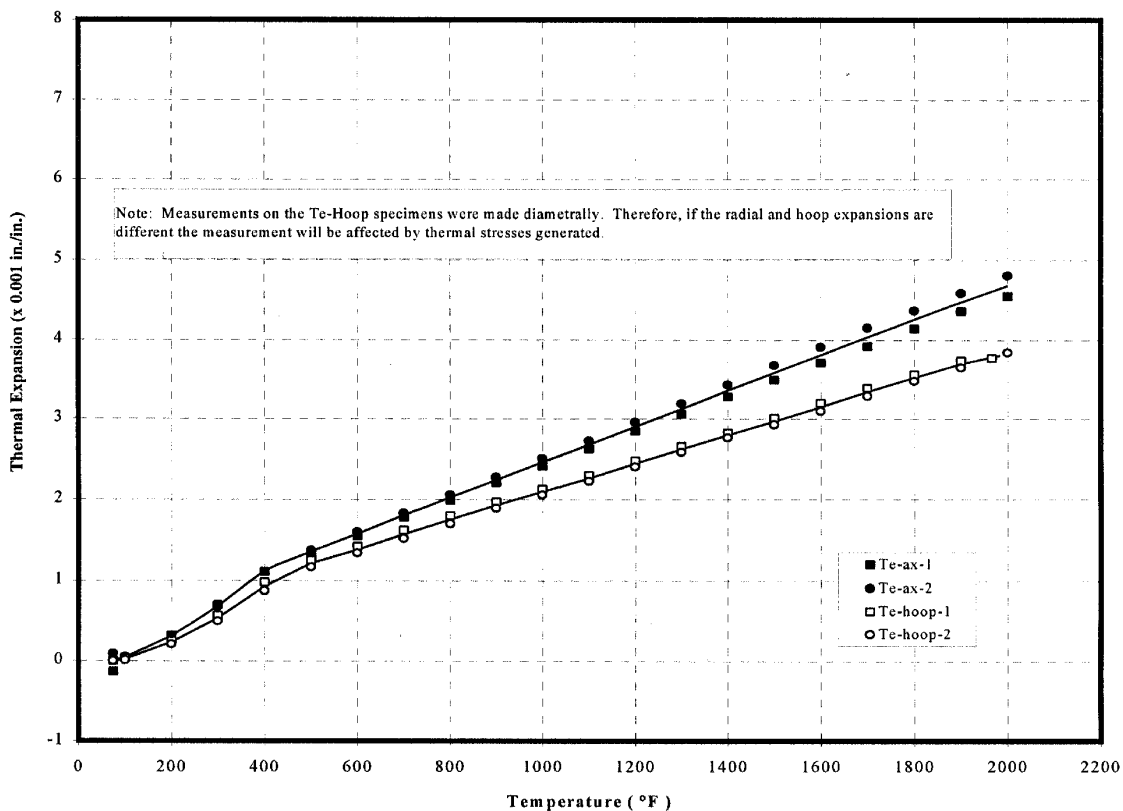


Figure 2. Thermal Expansion of Dupont/Lanxide PRD-66C

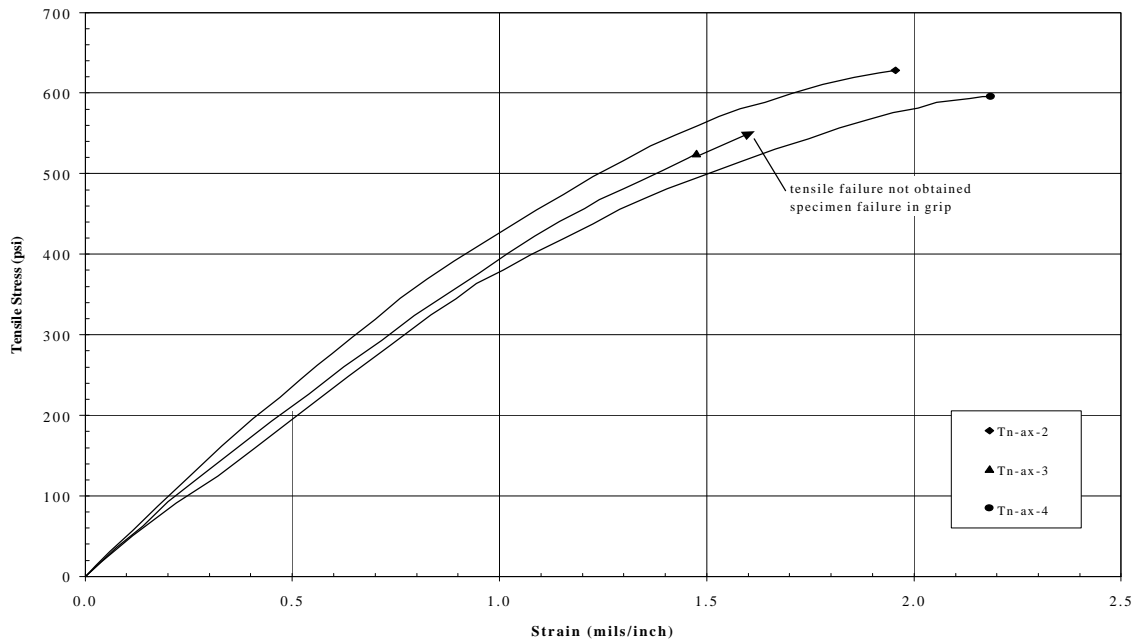


Figure 3. Axial Tensile Stress-Strain Responses of McDermott Ceramic Composite

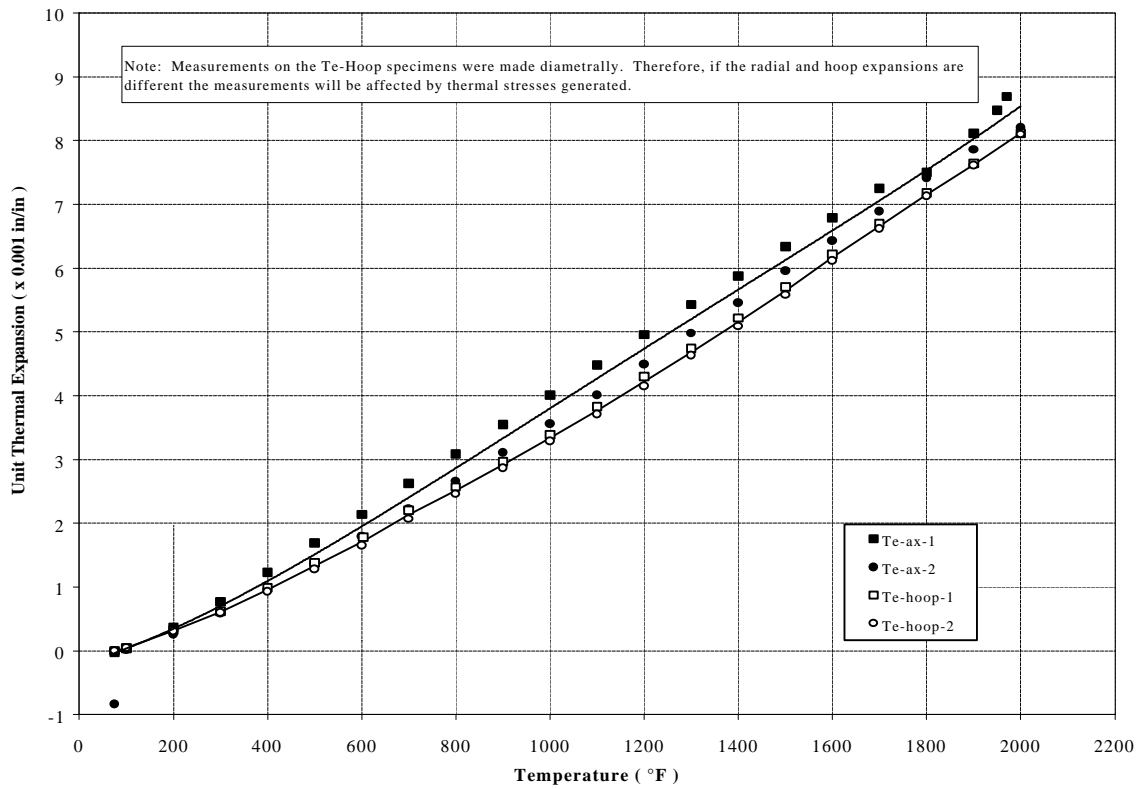


Figure 4. Thermal Expansion of McDermott Ceramic Composite

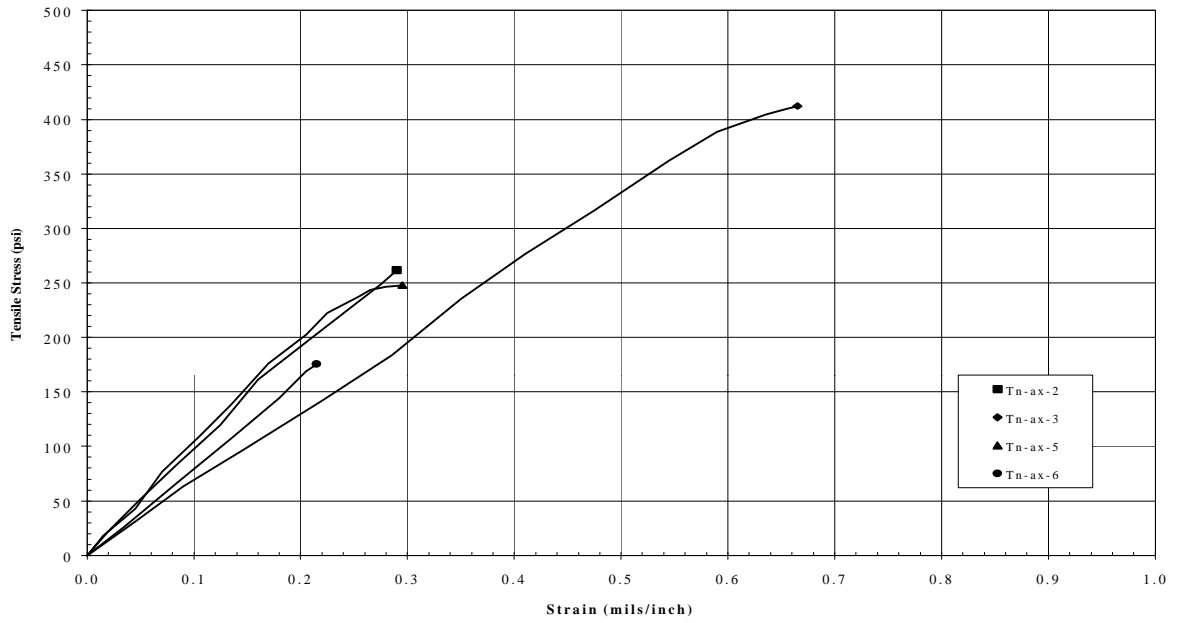


Figure 5. Axial Tensile Stress-Strain Responses of Blasch Precision Ceramics 4-270

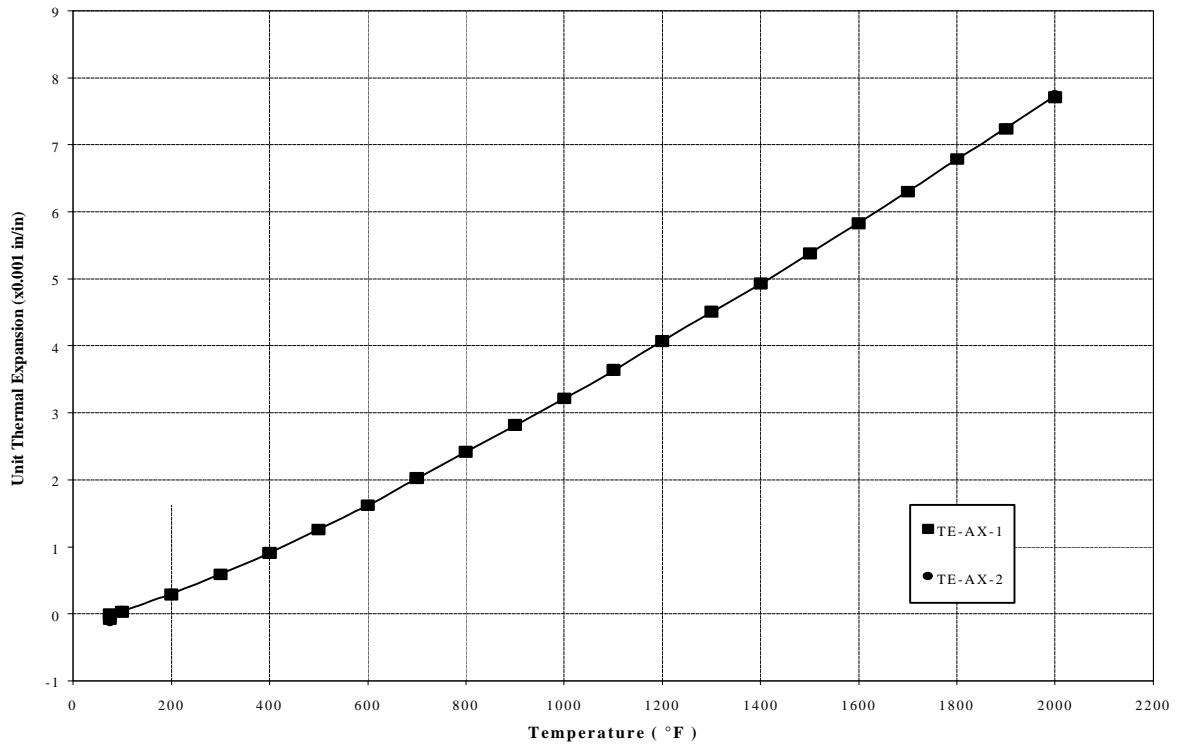


Figure 6. Axial Thermal Expansion of Blasch Precision Ceramics 4-270

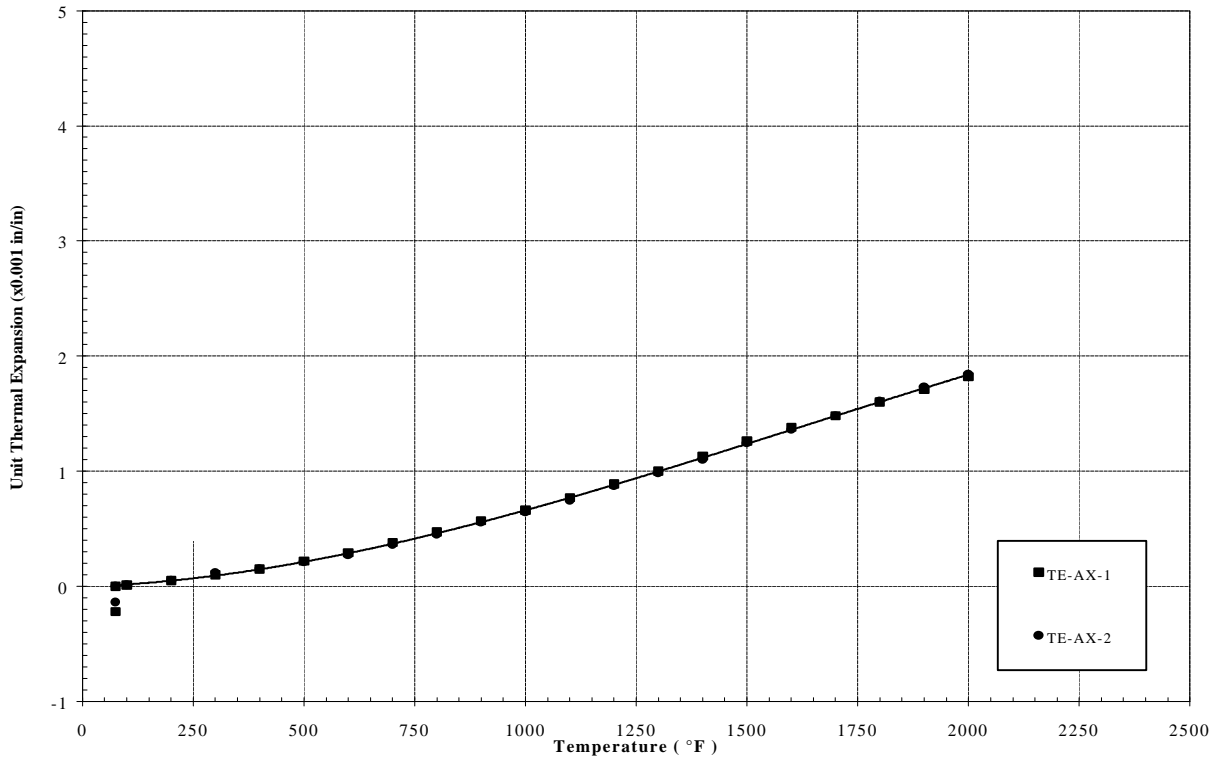


Figure 7. Axial Thermal Expansion of Specific Surface Cordierite

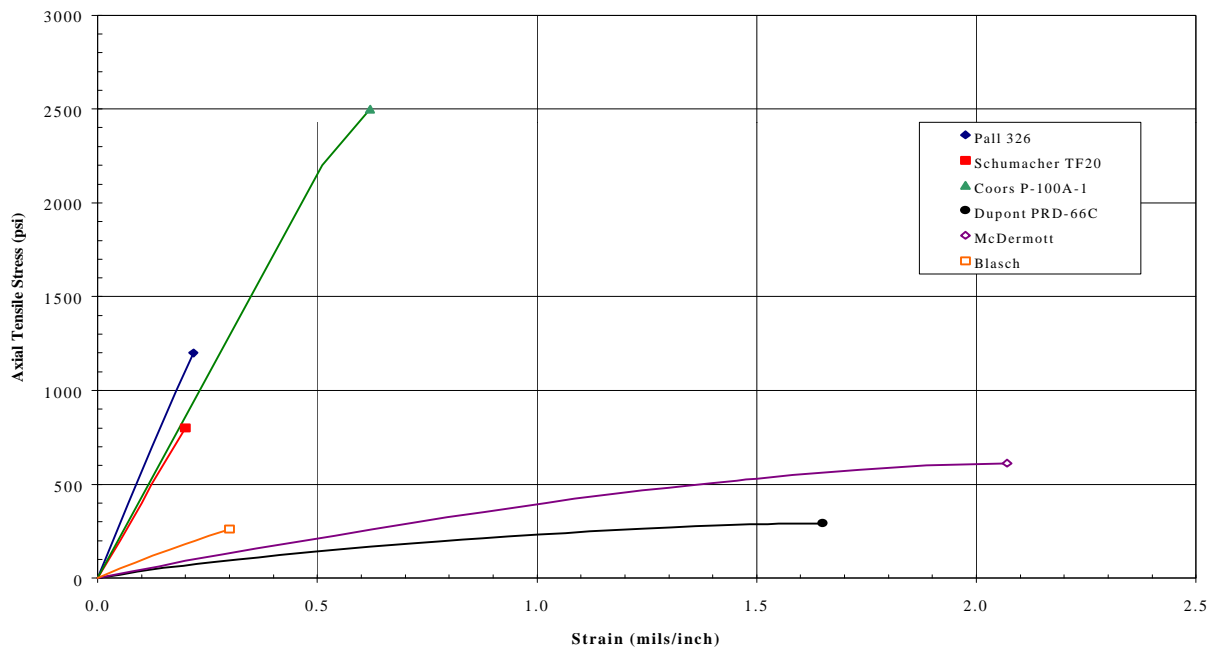


Figure 8. Probable Value Axial Tensile Stress-Strain Responses at Temperature

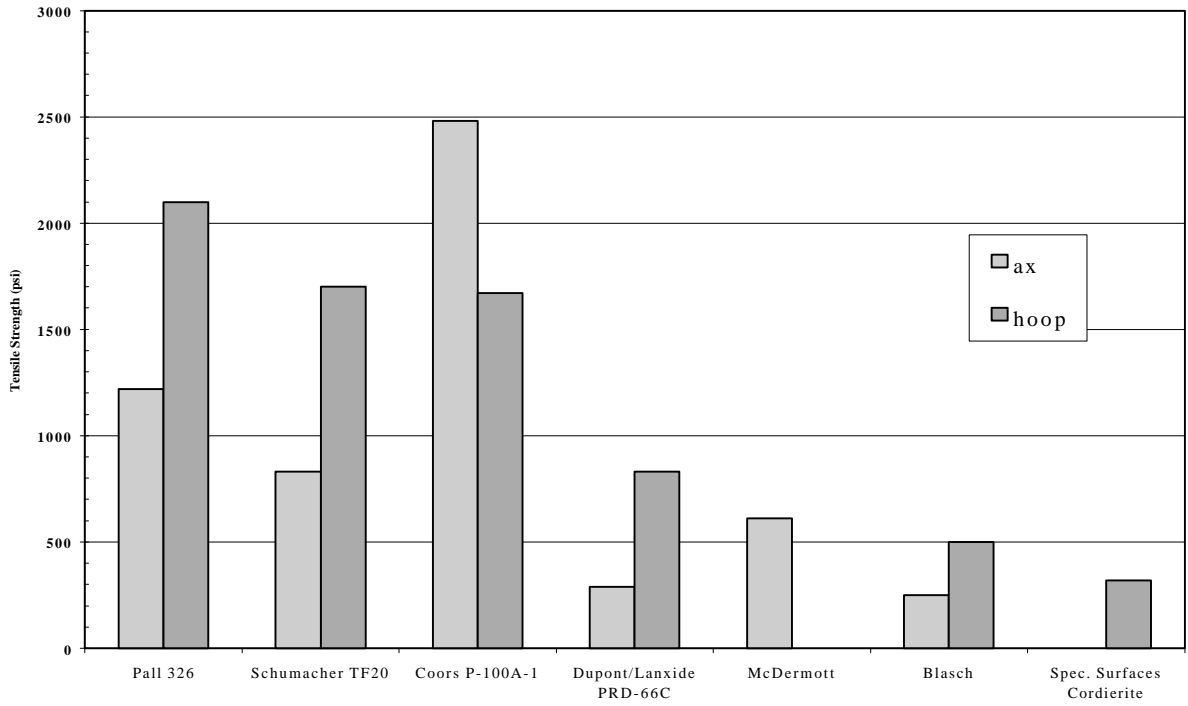


Figure 9. Room Temperature Tensile Strength of Several Candle Filter Materials

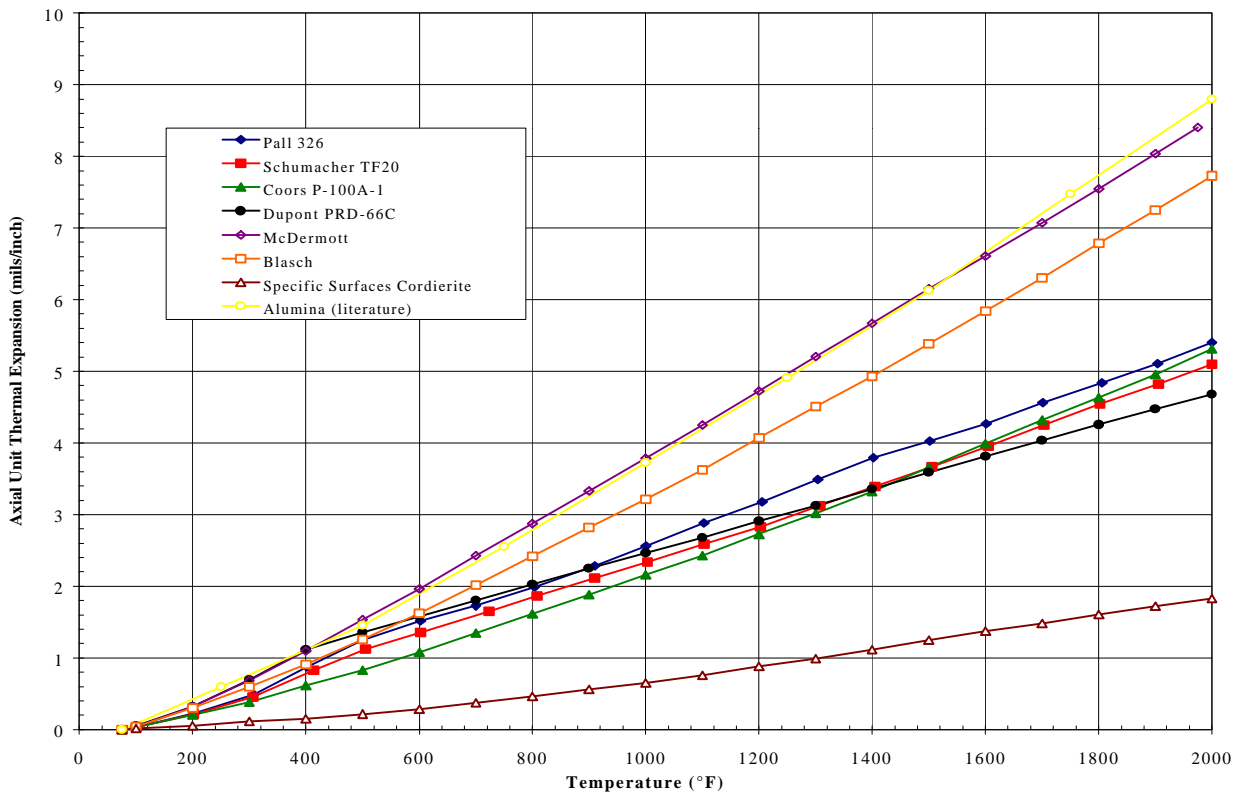


Figure 10. Axial Thermal Expansion of Several Candle Filter Materials

**Table 1**  
**Critical Material Issues for Candle Filters**

<b>Installation and Handling</b>	<b>Process Upsets (thermal stress and other loads)</b>	<b>Life (creep, static fatigue, degradation)</b>	<b>Pulse Cleaning (thermal stress)</b>
Tensile strength “Toughness”	Thermal expansion Tensile strain-to-failure Thermal conductivity Tensile Strength “Toughness”	Creep Static fatigue/crack propagation Degradation	Thermal Expansion Tensile strain-to-failure “Toughness”

**Table 2**  
**Test Matrix for PRD-66C, McDermott Ceramic Composite, Specific Surfaces Cordierite, and Blasch Precision Ceramics Candle Filters**

<b>Material</b>	<b>Test</b>	<b>Replications at Temp. (°F)</b>	
		<b>RT</b>	<b>1800</b>
<b>Dupont PRD-66C</b>	Tn-hoop	18	
	Tn-axial	6	
	TE-axial	2----->	
	TE-hoop	2----->	
	K-radial	2----->	
	Tn creep – ax	3 (temperatures TBD)	
	Microscopy	X	
<b>McDermott</b>	Tn-hoop	9	
	Tn-axial	3	
	TE-axial	2----->	
	TE-hoop	2----->	
	K-radial	2----->	
	Tn creep – ax	3 (temperatures TBD)	
	Microscopy	X	
<b>Specific Surface</b>	Tn-hoop	4	
	Tn-axial	5	
	TE-axial	2----->	
	TE-hoop	2----->	
	K-radial	2----->	
	Tn creep – ax	3 (temperatures TBD)	
	Microscopy	X	
<b>Blasch</b>	Tn-hoop	9	
	Tn-axial	4	
	TE-axial	2----->	
	K-radial	2----->	
	Tn creep – ax	3 (temperatures TBD)	
	Microscopy	X	

Legend: Tn - tensile, TE - thermal expansion, K – thermal conductivity

**Table 3**  
**Summary of Axial Tensile Results for Dupont/Lanxide**  
**PRD-66 Candle Filter Material**

Filter Identification	Specimen Number	Test Temperature (°F)	Specimen I.D. (in.)	Specimen O.D. (in.)	Ultimate	Young's	Strain-to Failure (mils/in.)	Notes
					Tensile Strength (psig)	Modulus (msi)		
C631	Tn-Ax-1	RT	1.75	2.35	280	0.38	1.40	Failed at end of grips
C631	Tn-Ax-2	RT	1.74	2.35	290	0.35	1.56	
C631	Tn-Ax-3	RT	1.74	2.35	290	0.36	1.59	Failed at end of grips
C638	Tn-Ax-4	RT	1.74	2.33	270	0.35	1.22	Failed at end of grips
C638	Tn-Ax-5	RT	1.73	2.34	280	0.30	1.57	Failed at end of grips
C638	Tn-Ax-6	RT	1.73	2.34	<del>290</del> 283	<del>0.34</del> 0.35	<del>1.74</del> 1.51	

**Table 4**  
**Summary of Hoop Tensile Results for Dupont/Lanxide**  
**PRD-66 Candle Filter Material**

Filter Identification	Specimen Number	Test Temperature (°F)	Specimen I.D. (in.)	Specimen O.D. (in.)	Maximum Hydrostatic Pressure (psig)	Isotropic	Anisotropic	Anisotropic		Strain-to-Failure	
						Ultimate Tensile Strength <sup>1</sup> (psi)	Ultimate Tensile Strength <sup>2</sup> (psi)	Young's Modulus <sup>2</sup> at I.D. (msi)	0°	90°	0°
C631	Tn-Hoop-1	RT	1.75	2.35	193	680	1130				
C631	Tn-Hoop-2	RT	1.74	2.35	191	660	1080	3.2	3.2	>0.18	>0.30
C631	Tn-Hoop-3	RT	1.75	2.36	249	860	1440				
C631	Tn-Hoop-4	RT	1.75	2.35	249	870	1440				
C631	Tn-Hoop-5	RT	1.74	2.36	220	750	1280				
C631	Tn-Hoop-6	RT	1.74	2.35	239	830	1390				
C631	Tn-Hoop-7	RT	1.75	2.35	250	870	1450				
C631	Tn-Hoop-8	RT	1.75	2.35	195	670	1140	3.1	3.1	>0.39	>0.24
C631	Tn-Hoop-9	RT	1.74	2.35	238	820	1380				
C638	Tn-Hoop-10	RT	1.73	2.34	258	870	1490				
C638	Tn-Hoop-11	RT	1.75	2.35	221	770	1280	3.7	1.2	>0.25	1.02
C638	Tn-Hoop-12	RT	1.74	2.34	278	950	1610				
C638	Tn-Hoop-13	RT	1.74	2.34	253	880	1460				
C638	Tn-Hoop-14	RT	1.74	2.34	253	890	1470				
C638	Tn-Hoop-15	RT	1.74	2.33	270	950	1570				
C638	Tn-Hoop-16	RT	1.73	2.34	271	920	1570				
C638	Tn-Hoop-17	RT	1.73	2.36	237	790	1370	3.1	2.8	0.47	0.48
C638	Tn-Hoop-18	RT	1.73	2.34	<del>271</del> 241 27	<del>930</del> 831 93	<del>1570</del> 1396 158				
					11%	11%	11%				

Notes: 1. Isotropic stress calculations by Lamé's solution  
2. Anisotropic stress calculations as given by Lekhnitskii

**Table 5**

**Summary of Hoop Tensile Results for McDermott Candle Filter Material**

Filter Identification	Specimen Number	Test Temperature (°F)	Specimen I.D. (in.)	Specimen O.D. (in.)	Maximum Hydrostatic Pressure <sup>1</sup> (psig)	Isotropic Maximum Tensile Stress <sup>2</sup> (psi)	Anisotropic Maximum Tensile Stress <sup>3</sup> (psi)	Anisotropic Young's Modulus <sup>2</sup> at I.D. (msi)		Strain-to-Failure (mils/in.)	
								0°	90°	0°	90°
8-1-23	Tn-Hoop-1	RT	1.96	2.43	>90	>420	>540				
8-1-23	Tn-Hoop-2	RT	1.94	2.36	>105	>540	>670	0.7			
8-1-23	Tn-Hoop-3	RT	1.94	2.39	>107	>520	>650				
8-1-23	Tn-Hoop-4	RT	1.95	2.36	>110	>590	>710				
8-1-23	Tn-Hoop-5	RT	1.94	2.38	>99	>490	>620				
8-1-23	Tn-Hoop-6	RT	1.94	2.36	>97	>500	>610				
8-1-23	Tn-Hoop-7	RT	1.94	2.36	>108	>560	>690				
8-1-23	Tn-Hoop-8	RT	1.94	2.34	>121	>580	>760	1.0	1.1	0.75	0.81
8-1-23	Tn-Hoop-9	RT	1.96	2.43	>124	>580	>750				
					>107	>530	>670				

Notes: 1. Tensile failure was not obtained because the yarns pulled out. The values shown were the maximum values measured before pullout occurred. A longer specimen is required to obtain tensile failure.

2. Isotropic stress calculations by Lamé's solution

3. Anisotropic stress calculations as given by Lekhnitskii

**Table 6**

**Summary of Axial Tensile Results for Blasch Precision Ceramics Candle Filter Material**

Filter Identification	Specimen Number	Test Temperature (°F)	Ultimate Tensile Strength (psi)	Young's Modulus (msi)	Strain-to-Failure (mils/in.)	Notes
BPC-B14	Tn-ax-1					Broke during machining
BPC-B14	Tn-ax-2	RT	260	0.96	0.30	
BPC-B14	Tn-ax-3	RT	410	0.67	0.67	
BPC-B14	Tn-ax-4	RT				Broke during machining
BPC-B14	Tn-ax-5	RT	250	1.03	0.30	
BPC-B14	Tn-ax-6	RT	175	0.81	0.22	

**Table 7**

**Summary of Hoop Tensile Results for Blasch Precision  
Ceramics Candle Filter Material**

Filter Identification	Specimen Number	Test Temperature (°F)	Specimen I.D. (in.)	Specimen O.D. (in.)	Maximum Hydrostatic Pressure (psig)	Ultimate Tensile Strength (psi)	Notes
BPD-B14	Tn-Hoop-2	RT	1.44	2.37	99	220	
BPD-B14	Tn-Hoop-3	RT	1.45	2.36	138	300	
BPD-B14	Tn-Hoop-4	RT	1.51	2.35	210	510	
BPD-B14	Tn-Hoop-5	RT	1.52	2.36	210	520	
BPD-B14	Tn-Hoop-6	RT	1.51	2.37	175	420	
BPD-B14	Tn-Hoop-7	RT	1.56	2.37	186	470	
BPD-B14	Tn-Hoop-8	RT	1.56	2.37	191	490	
BPD-B14	Tn-Hoop-9	RT	1.56	2.36	<del>218</del>	<del>560</del>	
					178	436	
					41	118	
					23%	27%	

**Table 8**

**Summary of Hoop Tensile Results for Specific Surfaces  
Cordierite Candle Filter Material**

Filter Identification	Specimen Number	Test Temperature (°F)	Specimen I.D. (in.)	Specimen O.D. (in.)	Maximum Hydrostatic Pressure (psig)	Ultimate Tensile Strength (psi)	Young's Modulus at I.D. (msi)		Strain-to-Failure (mils/in.)		Notes
							0°	90°	0°	90°	
							3	Tn-Hoop-1	RT	1.98	
3	Tn-Hoop-2	RT	1.98	2.40	53	270					
3	Tn-Hoop-3	RT	1.98	2.39	10	50					specimen adjacent to "stiffener"
3	Tn-Hoop-4	RT	1.98	2.40	7	30					specimen adjacent to "stiffener"

**Table 9**  
**Properties of Candle Filter Materials**

	<b>Pall 326</b>	<b>Schumacher TF20</b>	<b>Coors P- 100A-1</b>	<b>Dupont PRD- 66C</b>	<b>McDermott Ceramic Composite</b>	<b>Blasch 4-270</b>	<b>Specific Surface Cordierite</b>
<b>RT Axial Tensile Strength, psi</b>	1220	830	2480	290	610	250	
<b>RT Axial Young's Modulus, msi</b>	5.7	4.0	4.3	0.35	0.45	0.80	
<b>RT Axial Strain-to- Failure, in/in</b>	0.23	0.21	0.62	1.65	2.10	0.30	
<b>RT Hoop Tensile Strength, psi</b>	2100	1700	1800	830		500	320
<b>RT Hoop Young's Modulus, msi</b>				3.2	1.0		
<b>Maximum Hydrostatic Pressure, psig</b>	860	660	680	240		200	60
<b>Average Axial CTE 500 – 1500 °F, in/in/°F</b>	2.8	2.5	2.8	2.2	4.6	4.1	1.0
<b>Thermal Conductivity at 1000 °F, BTU-in/hr-ft<sup>2</sup>- °F</b>	38	52	11				